Study of interface dynamics of SP6/ZnO

Pietro Cataldi
pietro.cataldi0@gmail.com

2013-Set-01

Contents

Chapter 1

Theoretical introduction

In this chapter the basic background needed to understand the experimental data is given to the reader. The starting point will be a general introduction about the organic-inorganic interfaces with a focus on the single materials used in the experiment: SP6 and ZnO. Then the concept of excitons will be introduced with particular attention to the dynamics of this particles at interfaces and the possibility of charge transfer. In the last section our junction composed by SP6 deposed on ZnO will be presented, explaining what already is known and what we would like to determine with our analysis.

1.1 Organic-inorganic interfaces

The integration of organic and inorganic semiconductors in a hybrid structure has a big potential for optical and electronic applications. In fact, organic materials typically exhibit high yield of fluorescence, large absorption cross section and a good spectral tunability, while inorganic semiconductors are known for the large charge carrier mobilities. The combination of these properties would enhance the performance of devices, such as light-emitting diodes and photovoltaic cells. A fundamental requirement to make this concept work is to have an efficient coupling between the electronic excitation of the two types of materials [BSH08]. Typically these excitations are modeled with the aid of the theory of the excitons, which will be presented in section 1.4. The next sections present the organic and inorganic materials studied in this work.

1.2 SP6 or 2,7-bis(biphenyl-4-yl)-2,7-di-tert-butyl-9,9-spirobifluorene

SP6 is a spirobifluorene derivative. The spiro linkage visible in figure 1.1 of SP6 prevents crystallization and therefore, when these molecules are deposited on the surface, they form an amorphous layer [BSH08].

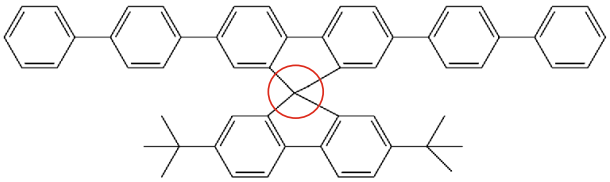

Figure 1.1: SP6 molecular structure. The spiro linkage is highlighted by the red circle. Is possible to see the benzene and the methyl structure. Figure from [BSH08].

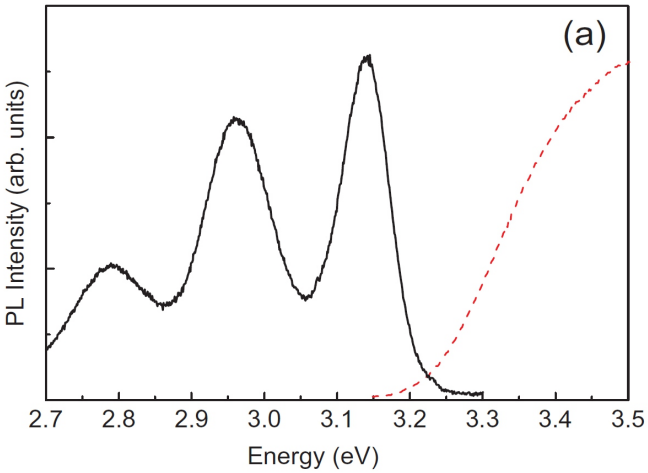

Figure 1.2: Photoluminescence (solid line) and Photoluminescence Exciton (dashed line) of a sole SP6 film inserted in between of two ZnO layers. Figure from [BSH08].

The morphological, structural and electronic properties of an organic/inorganic interface similar to the one studied in this work are presented in the work by Blumstengel et al. [BSH08]. They have found by means of optical spectroscopy, in particular with Photoluminescence technique, that the photoluminescence start around 3.3 eV as shown in figure 1.2. Here , using Photolumiscence Excitation (PLE), they have found that the absorption of the molecule have a maximum around 3.5 eV. Therefore the high occupied molecular orbital (HOMO) - lowest unoccupied molecular orbital (LUMO) band gap of the SP6 is in the order of 3.6 eV 1.3.

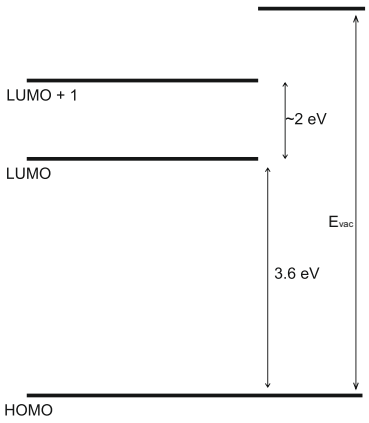

Figure 1.3: SP6 energy level diagram. The HOMO-LUMO band gap is 3.6 eV, while the band gap between LUMO and LUMO+1 should be in the order of 2 eV.

1.3 Zinc oxide: an adaptable material

Metal oxides are very common and ordinary on Earth - only gold has the property not to form an oxide on its surface when exposed to the air. As a result, trying to understand the physical and chemical properties of oxide surfaces is a topic of general interest and, of course, also a prerequisite for many applications [WÖ7]. In particular ZnO is becoming a relevant material since [KFZ$^+$10]:

- It is a candidate to btain a material for optoelectronics covering the spectral range from the green over the blue to the near UV, especially to obtain light emitting diodes (LED) or laser diodes (LD) in these spectral ranges. Concerning this argument was shown that, by alloying, the band-gap of the ZnO can be tuned from 2.8 to 4 eV [Ami12].

- It can be used as ZnO:Y(with Y that could be Al but also In or Ga) as a highly conductive transparent oxide (TCO). This can lead to the design of transparent components for electronic application.

- It can be used in solar cells. As will be explained in this section, ZnO is a convenient material to be used for this kind of technologies due to its salient characteristics such as low cost, easy synthesis, non-toxicity, high stability, and good optoelectronic properties [HYZ11].

In this section the structure and the optoelectronic properties of ZnO are illustrated. This material is a wide direct band gap semiconductor with $E_g(0°K) \approx 3.44eV$ and $E_g(300°K) = 3.37eV$. It belongs to the group of IIb-VI compound semiconductors. Compared to similar IIb-VI or III-V semiconductors it has a relatively strong polar binding and a comparably large exciton binding energy of $59.5meV$ [KFZ$^+$10]. This is one of the reasons that make ZnO so attractive for optoelectronic devices. High exciton binding energy materials give brighter emissions, because the exciton is already a bound system, which radiatively recombines with high efficiency without requiring traps to localize the carriers [Ami12].
ZnO can crystallize in three forms: hexagonal wurtzite, cubic zincblende, and the rarely observed cubic rocksalt. The hexagonal wurtzite structure is the most common phase (see fig. 1.4). In this case, each Zn^{2+} ion is surrounded by a tetrahedron of four O ions, and vice versa. This structure can be described schematically as a number of alternating planes of O and Zn ions stacked along the c-axis [DBD02].

The ZnO structure has non-polar surfaces $(11\bar{2}0)$ and $(10\bar{1}0)$, and polar (0001) and $(000\bar{1})$ [DBD02]. The non-polar surfaces are formed by breaking the same number of oxygen and zinc bonds and they contain an equal number of O and Zn ions, whereas the polar surfaces are either Zn(0001) or O$(000\bar{1})$ terminated. The two polar ZnO surfaces are the most important ones from the applied point of

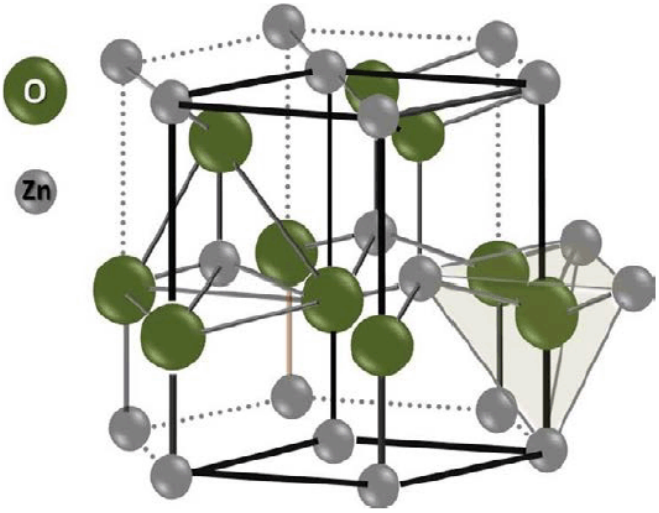

Figure 1.4: ZnO wutzite structure. Figure from [Ami12].

view. The polar surfaces of ZnO are highly metastable in nature and is responsible for several properties including piezoelectricity [Ami12] and has been reported to be the active crystal plane in methanol synthesis [DBD02].

Other favorable aspects of ZnO are that it is non-toxic, cheap, relatively abundant on earth, that it can be synthesized as a large single crystal by various methods and it can be grown in various morphologies and dimensions, for example as a quantum well (QW) or a quantum rod [Ami12].

Typically ZnO is n-type doped. Replacing Zn atoms with group III elements it is easy to create doping levels up to $n = 10^{21} cm^{-3}$. Doping ZnO p-type is notoriously difficult. Group I elements (Li, Na, K) replacing Zn form deep acceptors, resulting in high resistivity material but not in efficient p-type conductivity. Group V elements (N, P, As,Sb) instead of O result sometimes in p-type conductivity sometimes also in n-type [KFZ$^+$10].

This material exhibits also a quite hight electronic transport. The mobility in bulk samples, epilayers or nanorods is about 200 to 500 $cm^2/(Vs)$ at room temperature, limited by the intrinsic phonon scattering process. It goes with decreasing temperature through a maximum of a few 1000 $cm^2/(Vs)$ around $100°K$ and decays at lower temperature due to scattering with impurities. In quasi two-dimensional QWs and heterojunctions, this latter process can be reduced and values between 3000 and 10000 $cm^2/(Vs)$ have been obtained in the $1°K$ temperature region. The hole mobility is generally considerably lower than the electron mobility. Typical values reported at room temperature range from a few to some tens of $cm^2/(Vs)$ [KFZ$^+$10].

For many of the application described above, it is very important to consider the creation of electron-hole pairs when light shines onto the sample. Excitons play an important role in understanding what is really happening on the microscopic level.

1.4 Excitons

The exciton is the fundamental optical excitation of a material. It can be created for example in a semiconductor, when a photon is absorbed and excites an electron to the conduction band. This electron leaves a hole behind. The definition of the exciton comes into play when this electron-hole pair is considered as a single neutral particle. Depending on the localization of the electron-hole pair, one distinguishes between three kinds of excitons: The Frenkel, the Wannier and the Charge Transfer (CT) excitons.

- For the small-sized Frenkel excitons found in weakly bound molecular crystals, electron and hole are located on the same molecule[Fre31].
- In contrast, for the Wannier exciton, the relative motion of the electron and hole constituting the exciton encompasses hundreds of unit cells [Wan37].
- The last type is in between the two precedent configurations. This kind of excitons are formed in presence of an interface. The bounded electron and hole can be located in spatially separate regions across the interface of two different materials. In this case the exciton posses a dipole momentum [ZYM09].

The next sections present in more detail the theory behind the Wannier and the Frenkel exciton models and briefly present the CT exciton.

1.4.1 Frenkel Excitons

The Russian theorist Yakov Frenkel introduced the concept of excitation waves in crystals and invented the term exciton in 1936. By definition an exciton is an electron-hole pair correlated via Coulomb interaction, analog to the case of an ion in a perfect crystal, that differs from the others only by being in an excited electronic state [Fre31]. Frenkel treated the crystal potential as a perturbation to the Coulomb interaction between an electron and a hole which belong to the same crystal cell. This model works best to describe organic molecular crystals. Unlike Wannier excitons (see next subsection 1.4.2), the binding energy of Frenkel

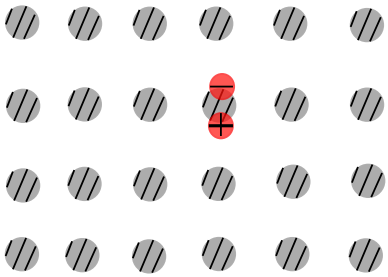

Figure 1.5: Scheme of the Frenkel exciton: it can be present only at distance of the order of 1 Å.

excitons can be of the order of the eV and the radius of interaction of the order of 1 Å. The excitation is localized on a single atom or very close to it (see fig. 1.5).

Essentially a Frenkel exciton is an excited state of a single atom, but the excitation can hop from one atom to another thanks to the coupling between neighboring atoms. The excitation wave travels through the crystal so that the translational states of Frenkel excitons have the form of propagating waves, like all other excitations in a periodic structure. If u_j is the ground state of atom j, the ground state of the crystal is

$$\psi_g = u_1 u_2 ... u_{N-1} u_N \tag{1.1}$$

The electronic structure of a crystal containing an exciton, can be described as a quantum mechanical superposition of states, in which it is equally probable for the excitation to be associated with any ion.

$$\phi_j = u_1 u_2 ... u_{j-1} v_j u_{j+1} ... u_N \tag{1.2}$$

Since excitons are non-distinguishable particles, this function has the same energy for any other atom excited. If there is any interaction between an excited atom and a nearby atom in its ground state, the excitation energy will be passed from atom to atom. We can express the Hamiltonian of the system as

$$H_{\phi_j} = \epsilon \phi_j + T(\phi_{j-1} + \phi_{j+1}), \tag{1.3}$$

where ϵ is the free atom excitation energy and T measures the rate of transfer of the excitation from j to its nearest neighbors. The solutions of this equation are Bloch waves and the energy eigenvalues are $E_k = \epsilon + 2Tcos(ka)$ [Kit05].

At present the Frenkel excitons are widely studied in organic materials where they dominate the optical absorption and emission spectra.

1.4.2 Wannier Excitons

The swiss Gregory Hugh Wannier has developed a concept of exciton in inorganic crystals, where the hopping rate of electron and hole between different crystal cells widely exceeds the strength of their Coulomb coupling. Wannier excitons have a typical size of the order of tens of lattice constants and a relatively small binding energy of typically a few meV (see fig. 1.6).

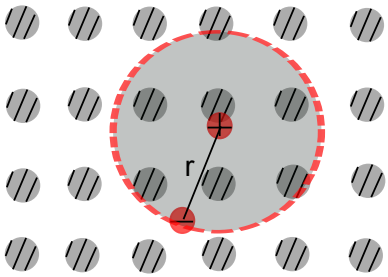

Figure 1.6: Scheme of the Wannier exciton: r could be in the range of several Å.

Such excitons can be conveniently described within the effective mass approximation, which allows to neglect the periodic crystal potential and to describe electrons and holes as free particles having a parabolic dispersion. These particles are characterized by effective masses which are dependent on the crystal material. The electrons in the excited state have effective mass m_c and the holes left behind have effective mass m_v. They interact through an attractive Coulomb interaction screened by the dielectric constant ϵ of the crystal. This is just the hydrogen atom problem, with the hydrogen atom reduced mass μ replaced by the reduced effective mass m^*

$$1/m^* = 1/m_c + 1/m_v \tag{1.4}$$

and the electronic charge replaced by e^2/ϵ.

This way, the energy of these bound states will be lower than the energy $\epsilon_c - \epsilon_v$ of the non-interacting electron and hole by

$$E_{ex} = \frac{m^* e^2}{m\epsilon^2 2a_0} = \frac{m^*}{m\epsilon^2}(13.6)eV \tag{1.5}$$

where a_0 is the Bohr radius, m is the mass of the electron and the constant of 13.6 eV come out from the hydrogen atom model.

The lowest of these bound states will have a new Bohr radius given by

$$a_{ex} = \frac{m\epsilon a_0}{m^*}. \tag{1.6}$$

The validity of this model requires that a_{ex} is large in comparison with a_0, but since insulators with small energy gaps tend to have small effective masses and large dielectric constants, this requirement is easily met, especially in semiconductors (see [AM76]).

What really happens in nature is unlikely so schematic as it is in our models. It was shown that the progress in material fabrication over the last years makes it feasible to manufacture hybrid semiconductor structures in which Wannier and Frenkel excitons are electronically coupled to each other. It has been theoretically predicted that such coupled excitons will exhibit unique features benefit from the specific advantages of the individual species and open up an avenue to a new class of optoelectronic applications [BSX$^+$06]. For these reasons the next section explains what can happen in a junction between different semiconductors, with a focus on what is already known to happen at a SP6/ZnO interface, which is of particular interest for this work.

1.4.3 Charge Transfer exciton

As seen in the precedents sections, a typical exciton consists of an electron and a hole located in the spatial region of the same material and possesses no dipole moment. If there is an interface the situation can be completely different. The electron and hole can be located in spatially separate regions across the interface and the result is a Charge Transfer (CT) exciton possessing a dipole momentum [ZYM09] see section 1.7.

CT excitons are currently considered as an important intermediate state in the creation of free carriers by light absorption (see paragraph 1.5).

What happens in nature is typically a mixture of the three possible excitons. CT exciton and Frenkel exciton become quite similar and can interact and mix as soon as the energetic difference between the two configurations is small. These mixed Frenkel-CT excitons show properties of both types of contributing states: The Frenkel exciton provides a large oscillator strength, whereas the CT exciton causes a high sensitivity to external electric fields [HSF$^+$00].

Such exciton mixed model is starting to have more ad more importance, since a rising number of new organic crystals form this kind of excited states and these crystals are important for thin film devices.

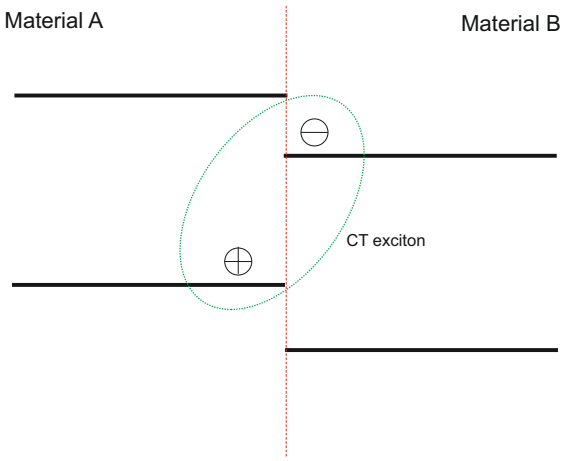

Figure 1.7: Scheme of the CT exciton: The dipole moment is generated across the interface.

Is interesting and useful to go more in the details on the creation mechanism of the charge transfer excitons. For this reason in the next section is explained how these particles are formed.

1.5 Charge Transfer

Charge transfer (CT) processes are important in many different scientific fields, e.g. physics, biology and chemistry. For example they play a crucial role in the creation of current in photovoltaic devices. Of particular interest is the study of the heterogeneous electron transfer (HET) which play a fundamental role in solid-molecular interfaces such as the one studied in this work (see section 1.6). HET is also involved in other technologically relevant fields such as nanoscale electronic devices, electrochemistry and many catalytic processes[St07].

Historically, many different approaches were used to describe CT processes. In this thesis the physics approach to describe CT by wave function overlap and tunnel processes will be presented. If the function overlap dominates we are talking about substrate-dominated charge transfer, while if the tunnel processes are more influential we talk of barrier-determined charge transfer.

The image potential of an electron at the interface is depicted in figure 1.8 a.

This image potential is formed because a charge particle brought near a conducting surface polarizes it; this allows for the electron to be bound in a potential well for a short period of time. Quantum mechanically, an electron bound near the surface can be described by discrete energy levels called Image Potential States and the interaction between the surface and the particles is mediated via a Coulomb-like potential. The corresponding wave function is also present in the figure, since it decays exponentially into the solid, the electron posses a non-zero residual probability to be found inside the solid due to the overlap of the wavefunctions. Therefore, the charge transfer time τ_{CT}, i.e. the decay time of the excited state back to the substrate, is strongly determined by the degree of overlap [EBC+04]. This kind of description for the charge transfer is strongly dependent on the surface electronic band structure and on the density of states. Therefore is called substrate-dominated [St07]. This kind of picture suits well for the description of relaxation of excited interfacial electrons, which are delocalized parallel to the surface plane, such as image potential states.

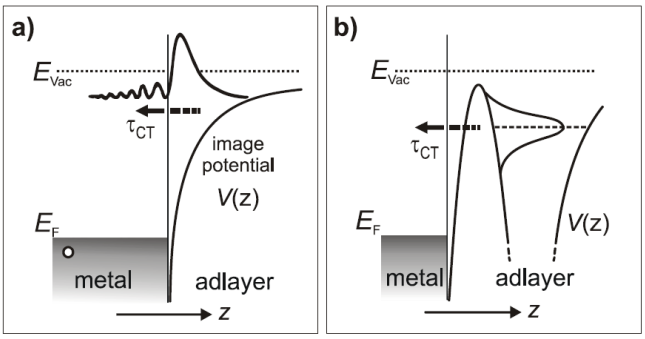

Figure 1.8: Charge transfer at the interface. (a): Substrate-dominated charge transfer. The image potential state exhibits a finite wave function overlap with the metal. This coupling determines the τ_{CT}. (b): Barrier-dominated charge transfer: The transfer time of an electron from a molecular orbital to the substrate is determined by the tuneling probability through the barrier. Figure from [St07].

On figure 1.8 b is possible to see the relaxation of electrons which are lightly coupled with the substrate as for example excited molecular orbitals [BGK+01]. In this case the reduced overlap of the wave function with the metal states is caused by a tunnel barrier present at the interface which diminishes the interaction be-

tween substrate and deposited layers [Gad95]. In this case the tunnel probability is the quantity which influence the rate of charge transfer. This means that τ_{CT} is prevalently determined by the tunnel probability for one electron to pass the barrier and the substrate's electronic properties play a minor role. For this reason this kind of HET is called barrier-determined charge transfer.

We have seen that the charge transfer of an excited interfacial electron strongly depends on the surface electronic band structure of the underlying substrate if the wave functions overlap, and therefore the coupling is sufficiently strong; on the other hand, if the electron is efficiently screened from the metal, charge transfer is determined by tunneling through an interfacial barrier that reduces the coupling to the substrate states. It is shown that this two antithetic models for describing the charge transfer mechanism, often are superposed one with the other with a kind of transition between these two regimes which can occur at molecule-metal interfaces [St07]. In the next section a junction in which this kind of processes could happen will be presented.

1.6 Utilities of the heterojunction

A heterojunction is the interface of two layers or regions of dissimilar materials. Such interface exhibits interesting and useful electronic properties associated with the discontinuity in the local band structure. As a result, such heterostructures have become important as basis for novel devices. The most important property of a semiconductor heterojunction is the relative position in energy of the bandgaps in the two semiconductors. This relative position determines the conduction-valence band discontinuities, and hence the effective barrier for electron or hole transport across the interface [Ter84].

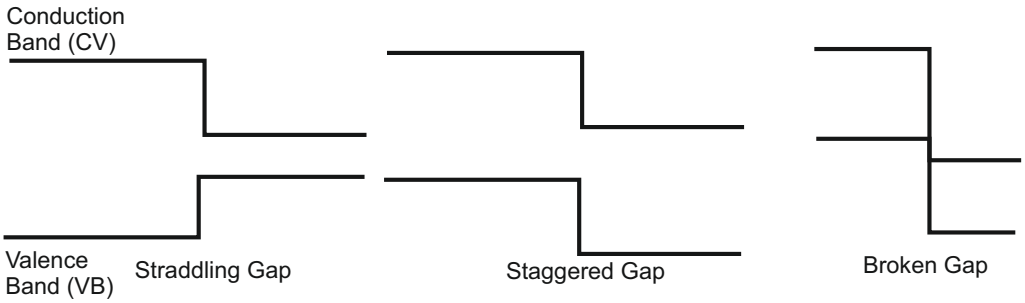

Figure 1.9: Scheme of the different possibility for heterojunctions.

Therefore, depending on the relative arrangement, there is the possibility to form different types of junctions, as depicted in figure 1.9 [Moe01]:

1. Type I or straddling junction (left of figure 1.9): the bandgap of one semiconductor is completely contained in the bandgap of the other one. The discontinuities of the bands are such that both types of carriers, electrons and holes, need energy to transfer from the material with the smaller band gap to the one with the larger gap, while it is easy to inject majority carriers from the wide band gap side to the other. For this reason this kind of junctions are more suitable for light emitting devices.

2. Type II or staggered junction (figure 1.9, center): the bandgaps overlap. The situation with respect to moving carriers from one side to the other or vice versa is no longer symmetrical. If one kind of carrier gains energy, for example moving from the right side of the junction to the left, the other one needs energy for a displacement in the same direction. For this reason, when an electron-hole pair is created it tends to separate and therefore this kind of junction is more suitable for photovoltaic applications, which rely on charge separation.

3. Type III or broken-gap junction (right of figure 1.9): the bandgaps lightly overlap or do not overlap at all. The situation for carrier transfer, after electron-hole pair creation, is similar to type II junction, just more pronounced.

This work studies the heterojunction between SP6 molecules and ZnO. It is a hybrid organic-inorganic structure, which forms a type-II junction where charge separation is more probable to occur at the interface. The energy level diagram for the SP6/ZnO interface is depicted in figure 1.10.

When an electron hole pair is created in the molecule, there is a high probability that an exciton is created also in the ZnO since the bandgap of the inorganic part is smaller than the band gap of the molecule. There are different behaviors for the created excitons in the inorganic part of the junction: they can recombine or they can reach the interface between the two materials and undergo charge separation. This process depends on the thickness of the molecular layers which are on the ZnO. In fact, as it is possible to see in fig. 1.11 the thicker the SP6 layers and the more possible it is to see an intense and time lasting photoluminescence. There is a quenching of the photoluminescence due to the fact that with a thinner SP6 layer is more easy for the photo-excitated electrons to reach the surface and to charge separate[BSH08] and not recombine. On the other hand if the thickness of the SP6 is higher the recombination will be more important and therefore the photoluminescence, which comes from the recombination, will be more intense and present for a longer time.

In [BSH08] the authors have measured the photoluminescence lifetime of the SP6 molecules and found that is $\tau_{pl} \approx 300ps$. In this article they were detecting

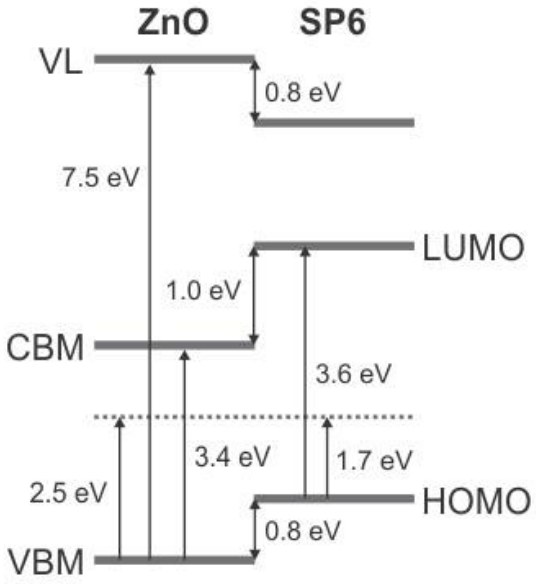

Figure 1.10: SP6/ZnO energy level diagram. Figure from [BSH08].

the photons emitted between the HOMO-LUMO level of the molecule with a resolution in the order of the picosecond time range.

The aim of the present work is to study the same system from a different point of view (see 2.3 and 2.2.3). Theoretically, with transient absorption and SFG measures is possible to have a true comprehension of what is happening to the photo-excited electrons. In fact, using these techniques, is possible to take in consideration the dynamics of the excitons recombination of the SP6, the dynamics of the excitons in the ZnO and the dynamics of the charges transfer on the interface. With these technique is possible to study directly the dynamics of the excited levels of the system. This is possible because with these technique permit to study phenomena which happen on the femtosecond timescale because the time resolution with the experimental setup used is on the order of 10 fs. Therefore is possible to look at the electrons suddenly after the excitation. Therefore the aim of this work is to go more in the details of the relaxation of the system, trying to look at it in a more complete and satisfactory way. This means that in the experimental part of this master thesis (see experimental part when done), the time constants of the charges transfer and the one relative to the electron-hole pairs dynamics of the ZnO are tried to be determined in addition to the recombination one which is already known to be in the picoseconds range.

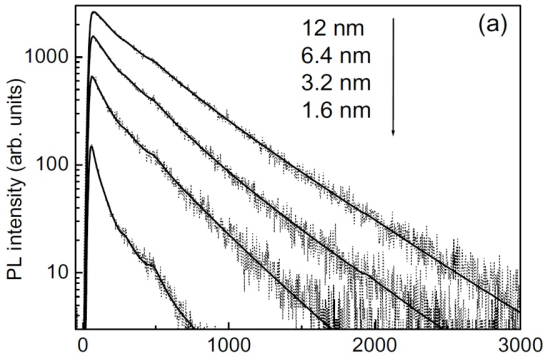

Figure 1.11: SP6/ZnO photoluminescence diagram . The thicker the deposited SP6, the harder it is for the electron-hole pair to separate and charge separate. This happens because it is more difficult for the charges to reach the surface. Figure from [BSH08].

Chapter 2

Experimental techniques

The theory behind our experimental technique is presented in this chapter. In particular light is introduced as an instrument useful to investigate different property of matter, specially with the analysis of both the linear and nonlinear polarization contribution of the shined material. Then is given a brief introduction to our experimental methods: Transient absorption measure and Sum Frequency Generation technique. Last but not least our experimental setup is described.

2.1 Our detection instrument: Light

??

When propagating light gets in contact with a material, there is a coupling between them, and the solid responds to the radiation, in terms of polarization $\mathbf{P}$:

$$\mathbf{P} = \mathbf{P}^{(1)} + \mathbf{P}^{(2)} + \mathbf{P}^{(3)} + \cdots = \mathbf{P}^{(1)} + \mathbf{P}_{NL} \tag{2.1}$$

which can be expressed as sum of different contributions. The first term $\mathbf{P}^{(1)}$ is the linear contribution to the polarization. For weak electric incident fields this is the major one, since the others are orders of magnitude smaller. The second term $\mathbf{P}_{NL}$ is the nonlinear polarization contribution and plays an important role when the sample is exposed to high intensity fields. Both of them will be described in the following sections.

2.1.1 Linear polarization contribution

In electromagnetism the electric displacement $\mathbf{D}$ is the quantity that describes how the applied electric field $\mathbf{E}$ changes the organization, the coupling and the spatial arrangement of the charges in the medium

$$D_i = \sum_j \epsilon_{ij} E_j. \tag{2.2}$$

where ϵ_{ij} is a symmetrical tensor of rank two. In the most common situations the relation between $\mathbf{D}$ and $\mathbf{E}$ is linear, as in the case of isotropic and homogeneous media, where ϵ_{ij} becomes a scalar. For this reason in a dielectric, the two vectors must have the same direction and so [LL60]

$$\mathbf{D} = \epsilon \mathbf{E} = \epsilon_0 \epsilon_r \mathbf{E} \tag{2.3}$$

the coefficient ϵ is the dielectric constant of the substance and is a function of its thermodynamical state. In a dielectric, $\mathbf{E}$ displaces the bound charges, inducing a local electric dipole moment. This displacement is the polarization. Therefore $\mathbf{D}$, $\mathbf{E}$ and $\mathbf{P}$ are related by

$$\mathbf{D} = \epsilon_0 \mathbf{E} + \mathbf{P}. \tag{2.4}$$

When 2.3 and 2.4 are compared, one obtains

$$\mathbf{P} = \epsilon_0 \epsilon_r \mathbf{E} - \epsilon_0 \mathbf{E} = \epsilon_0 \mathbf{E}(\epsilon_r - 1) \tag{2.5}$$

and defining $\epsilon_r - 1 = \chi$, it becomes

$$\mathbf{P} = \epsilon_0 \chi \mathbf{E} \tag{2.6}$$

where χ is called susceptibility and indicates the degree of polarization of a material in response to an applied field.

What said is valid since in general in a dielectric the charges are bounded. All the previous dissertation is different in a metal because of the unbounded electrons present. When an electromagnetic field is applied, an induction current is created. In the majority of cases, the relation between these two quantity can be assumed to be linear

$$j_i = \sum_j \sigma_{ij} E_j \tag{2.7}$$

where σ_{ij} is a symmetrical tensor of rank two, the conductivity tensor. In this discussion the temporal dependence of the polarization was not considered. In the next section this argument will be discussed.

Time-dependent polarization

In this section we want to take into account that the phenomena of polarization of a material irradiated with light is not happening instantaneously in response to an applied field. In other words, it is possible that the polarization has a time dependence. The following discussion will be restricted to isotropic materials, where ϵ and σ are scalar functions. Under these assumptions the more general formulation for the polarization as a function of time is

$$\mathbf{P}(t) = \int_0 \chi(t-\tau)\mathbf{E}(\tau)d\tau. \tag{2.8}$$

The polarization is a convolution of the electric field at previous times with time-dependent susceptibility. In a linear system, it is more convenient to make the Fourier transform and write this relation as a function of frequency. Because of the convolution theorem, the integral becomes a simple product:

$$\mathbf{P}(\omega) = \epsilon_0\chi(\omega)\mathbf{E}(\omega) \tag{2.9}$$

This frequency dependence of the susceptibility is equivalent to a frequency dependence of the permittivity. $\epsilon(\omega)$ completely describes the properties of the system and its response to the external field. It is a complex quantity defined as

$$\epsilon(\omega) = \epsilon_1(\omega) + i\epsilon_2(\omega) \tag{2.10}$$

Typically the quantity ϵ_1 describes how much the electric field polarizes the medium, while ϵ_2 describes absorption: when a material is transparent, ϵ_2 is zero, but it becomes important when absorption starts.

In general it is really complicated to calculate the dielectric permittivity theoretically and to use it to determine the optical properties of a material. For this reason different kinds of models are used to try to understand microscopically what happens to the measurable quantities. In particular, insulators and glasses show vibrational absorption at infrared wavelengths and electronic absorption in the ultraviolet region, while they are colorless and transparent in the visible region. Metals, on the other hand, are highly reflective in the infrared and visible region, due to the presence of free carriers, while their typical color is due to electronic interband absorption. The two most simple and frequently used models are the Drude and the Lorenz model, both based on the concept of dipole oscillators. In a solid, three types of dipole oscillators can be distinguished: the ones due to bound electrons, those due to the vibration of charged atoms and finally those due to free electrons [Fog11]. The Drude model considers the electrons as free while the Lorentz model considers the electrons as bound to the nuclei. Both the models will be explained in the next sections.

2.1.2 The Lorentz model

The most simple classical theory which describe the general optical properties of a solid insulator is the one from Lorentz. In this model is supposed that the solid is composed of charged particles which behave as classical harmonic oscillators with mass m, charge e and a proper frequency $\omega_0 = \sqrt{K/m}$, where K is the Hook constant. If an external field of frequency ω is present, a damping factor γ proportional to the velocity of the charge particle is introduced and the electric field **E** is considered in the y direction, the equation of motion is given by :

$$m\frac{d^2y}{dt^2} + m\gamma\frac{dy}{dt} + \omega_0^2 my = eE_0e^{-i\omega t}. \tag{2.11}$$

The solution of 2.11 is:

$$y = \frac{eE_0e^{-i\omega t}}{m[(\omega_0^2 - \omega^2) - i\gamma\omega]} \tag{2.12}$$

From 2.12 is possible to calculate the current density $J = Ne\frac{dy}{dt}$ where N is the number of oscillators per unit volume. Comparing this equation with $J = \sigma E$, it is possible to obtain σ and from this the other important optical quantities. From 2.12 is possible also to directly obtain the dipole moment per unit volume $P = Ney = \alpha E$ and from this the dielectric constant

$$\epsilon(\omega) = 1 + 4\pi\alpha = 1 + \frac{4\pi e^2 N}{m(\omega_0^2 - \omega^2) - i\gamma\omega}. \tag{2.13}$$

Here α is the tensor of polarizability and it is assumed that all the N oscillator per unit volume have the same resonance frequency ω_0. Splitting the real part from the imaginary on eq 2.13 one obtains:

$$\epsilon_1(\omega) = 1 + \frac{4\pi e^2 N}{m}\frac{1}{(\omega_0^2 - \omega^2)^2 + \gamma^2\omega^2} \tag{2.14}$$

$$\epsilon_2(\omega) = \frac{4\pi e^2 N}{m}\frac{\omega\gamma}{(\omega_0^2 - \omega^2)^2 + \gamma^2\omega^2} \tag{2.15}$$

The presence of the damping factor γ avoids the infinity in the dispersion curve of $\epsilon_1(\omega)$ and gives a finite spread to the absorption curve, which is a Lorentian [BG00].

To explain how 2.14 and 2.15 can describe and be used to obtain the fundamental optical properties of a solid, is useful to know what happen in general when light strikes a discontinuity in the medium in which is propagating. In figure 2.1 the three basic phenomena which light experience are illustrated.

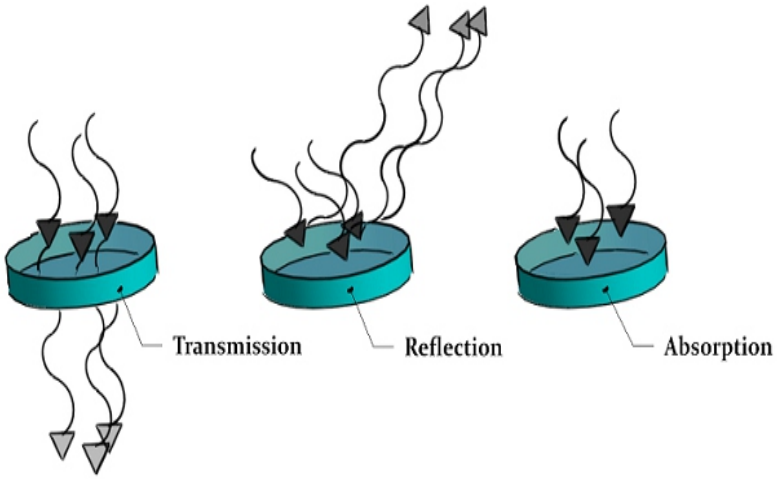

Figure 2.1: Different phenomena which happen when light hits an object: usually a mixture of these three phenomena happens. Figure from http://www.chroma.com/knowledge/introduction-fluorescence/transmission-reflection-and-absorption.

The wavelengths that pass through are said to be transmitted and the wavelengths that do not pass through are said to be blocked or attenuated. Blocking (attenuation) can be accomplished by reflecting or absorbing light by the filter object and the degree to which a filter transmits or attenuates light is completely dependent on its constituent materials. Is possible to have information on these processes analysing 2.14 and 2.15. In figure 2.2 the real and the imaginary part of $\epsilon(\omega)$ are depicted. Different regions demarcate by Roman number from I to IV are distinguishable. In each of this region reflection or absorption or transmission dominates. In fact is possible to connect 2.14 and 2.15 with the real and imaginary part of the refractive index, respectively n and k:

$$n^2 - k^2 = \epsilon_1 \tag{2.16}$$

and

$$2nk = \epsilon_2 \tag{2.17}$$

This means that from ϵ_1 and ϵ_2 it is possible to have n and k as a function of ω. n gives us information about the phase speed while k gives indication about the absorption of the material. They are represented in figure 2.3.

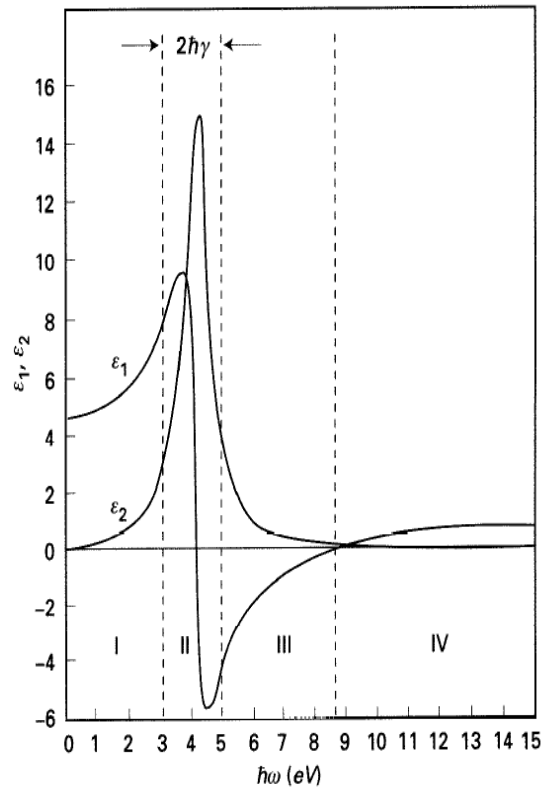

Figure 2.2: Real part and imaginary part of $\epsilon\omega$ in the Drude-Lorentz model.Here $\hbar\omega_0 = 4eV$ and $\hbar\gamma = 1eV$. Figure from [BG00].

We have seen how the knowledge of $\epsilon(\omega)$ can give us information about optical properties as transmission, reflection and absorption.

This model can be extended to the case of different Lorentz oscillators with resonance frequencies ω_j and damping coefficients γ_j. Each oscillator contributes to the dielectric constant with a strength f_j therefore extending equation 2.13 one obtains:

$$\epsilon(\omega) = 1 + \frac{4\pi e^2}{m} \sum_j \frac{f_j}{(\omega_j^2 - \omega^2) - i\omega\gamma_j} \tag{2.18}$$

In all this dissertation we where referring by to an insulator material.In the next section we will consider solid metal.

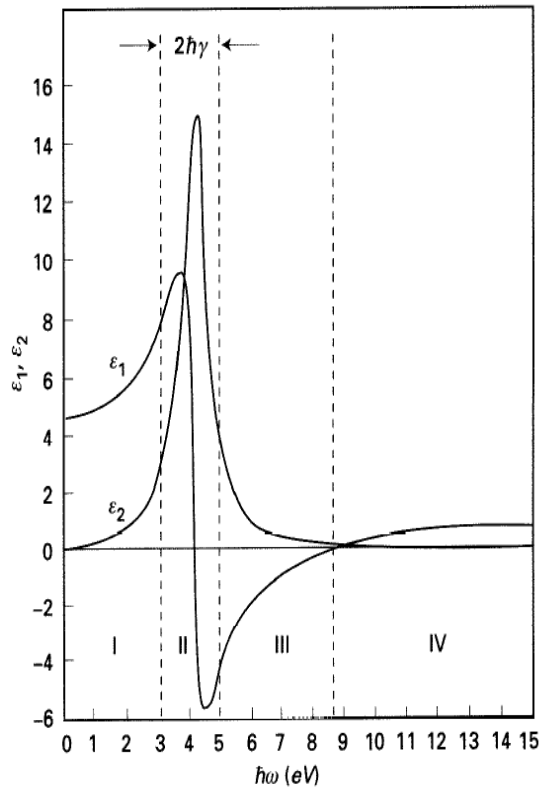

Figure 2.3: Spectral dependence of n and k from the data of ϵ_1 and ϵ_2 of figure 2.2. The region I is characterized principally by transmittance (T), the II by absorption (A), the III by reflectivity (R) and the IV by transmittance. Figure from [BG00].

2.2 Drude Model: optical properties of the metals.

For the treatment of the metal case is sufficient to impose $\omega_0 = 0$ in the equations 2.13-2.15. In this model is possible to define the plasma frequency as the eigen frequency of the collective longitudinal mode of the free electrons, for which $\epsilon(\omega_p) = 0$. It is:

$$\omega_p^2 = \frac{4\pi e^2 N}{m}, \tag{2.19}$$

and eq 2.14 and 2.15 become

$$\epsilon(\omega) = 1 - \frac{\omega_p^2}{\omega^2 + \gamma^2} + i\frac{\omega_p^2 \gamma}{\omega^3 + \omega\gamma^2} \tag{2.20}$$

Also in this case is possible to obtain, as in the precedent section, the conducibility σ and the current.

We will now discuss different behaviors as a function of frequency. In the limit of low frequency the conductivity can be written as (see [BG00]) (do you think i need to explain better? or may be use an appendix for the derivation of this formula?)

$$\sigma = \frac{\omega\epsilon_2}{4\pi} \approx \frac{\omega_p^2}{4\pi\gamma} = \frac{Ne^2}{m\gamma}. \tag{2.21}$$

Comparing 2.21 with the definition of the static conducibility

$$\sigma = \frac{Ne^2\tau}{m}. \tag{2.22}$$

one obtains

$$\gamma = \frac{1}{\tau} \tag{2.23}$$

Which means that the damping factor γ is related to the average time between collisions. The imaginary part $\epsilon_2(\omega)$ becomes important and the reflectivity is almost 1 for $\omega \ll 1/\tau$. In this case $\epsilon \approx i\epsilon_2$. Is possible to show (see [BG00]) that in this region the reflectivity goes like

$$R \approx 1 - 2\sqrt{\frac{\omega}{2\pi\sigma}} \tag{2.24}$$

Is can be seen that reflectivity goes to one with increasing value of σ untill the frequency is not too high in comparison with ω_p. Using equation 2.22 and 2.19 is possible to write eq 2.24 as

$$R \approx 1 - 2\sqrt{\frac{2\omega}{\omega_p^2\tau}} \tag{2.25}$$

In this region called relaxation region ($\omega \ll \omega_p$) the metal is still reflecting.

At higher frequency, ignoring the therm γ^2 with respect to ω^2, eq 2.20 gives

$$\epsilon_1 \approx 1 - \frac{\omega_p^2}{\omega^2} \tag{2.26}$$

and

$$\epsilon_2 \approx \frac{\omega_p^2\gamma}{\omega^3} \tag{2.27}$$

In this region the absorption $\eta = \frac{\omega\epsilon_2}{nc}$ is proportional to $1/\omega$. For $\omega \gg \omega_p$ equations 2.26 and 2.27 have limit $\epsilon_1 \to 1$ while $\epsilon_2 \to 0$. In this limit, the reflectivity tends to zero and the metal becomes transparent.

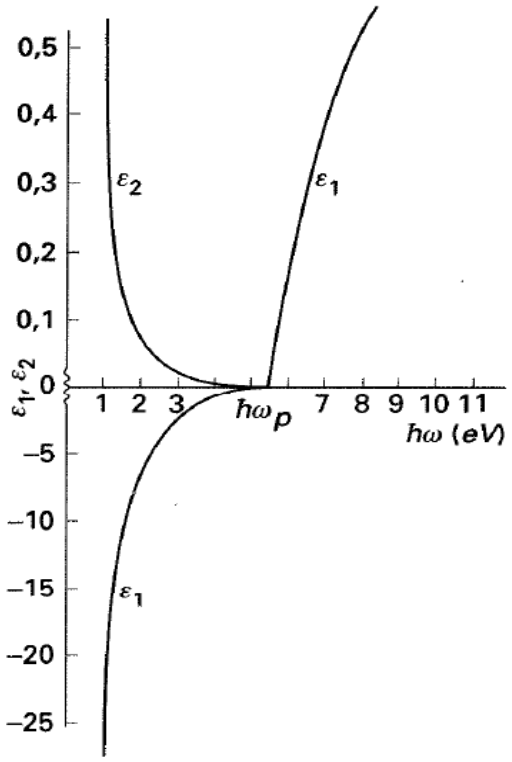

Figure 2.4: Spectral dependence of ϵ_1 and ϵ_2 for the free electron of a metal. ϵ_1 is always bigger than ϵ_2 except for $\omega \to 0$. Figure from [BG00].

ϵ_1 and ϵ_2 for a metal with free electrons are depicted in fig. 2.4 as a function of the frequency.

For the same model n and k as a function of ω are depicted in fig. 2.5. In comparison with the Lorentz model (fig. 2.3) for the free electrons the region I disappears while the region II of the heavy absorption is present only at very low frequencies. This discussion is based on classical physics. For more detailed understanding of what is really happening from a microscopical point of view, quantum mechanics has to be used.

2.2.1 Quantum mechanical point of view

In the quantum mechanical theory, light is composed by multiples of the fundamental quantum-wave particle: the photon. The electrons of the materials are disposed in a band structure and an incoming photon can cause the transition of a charged particle from a band to another. The probability for this transition is described by the Fermi golden rule as:

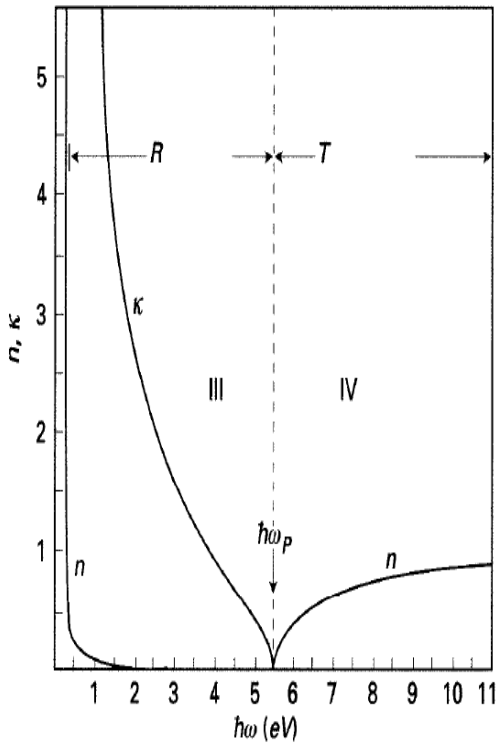

Figure 2.5: Spectral dependence of n and k for the free electron of a metal. The regions III and IV in analogy with fig. 2.3 are characterized with elevate values of reflectivity (R) and transparency (T). Figure from [BG00].

$$P = \frac{2\pi}{\hbar} |\langle f| H |i\rangle|^2 \rho \tag{2.28}$$

where $\hbar$ is the Plank constant, $\langle f| H |i\rangle$ is the matrix element of the Hamiltonian H with respect to the final state f and initial state i and ρ is the density of final state.

In general, in the quantum mechanical formalism, permittivity is related to atomic and molecular interactions and to changes of electronic states.

In a semiconductor at low frequencies of the incoming photon, a low number of electrons, in comparison with a metal, are available for conduction. When the energy of the incoming photon becomes comparable to the energy gap, it can excite an electron from an occupied state in the valence band to an unoccupied state in the conduction band (see 1.4). This is called an interband transition and is represented schematically in picture 2.6. In this process the photon is absorbed, an excited electronic state is formed and a hole is left behind. The relevant factors

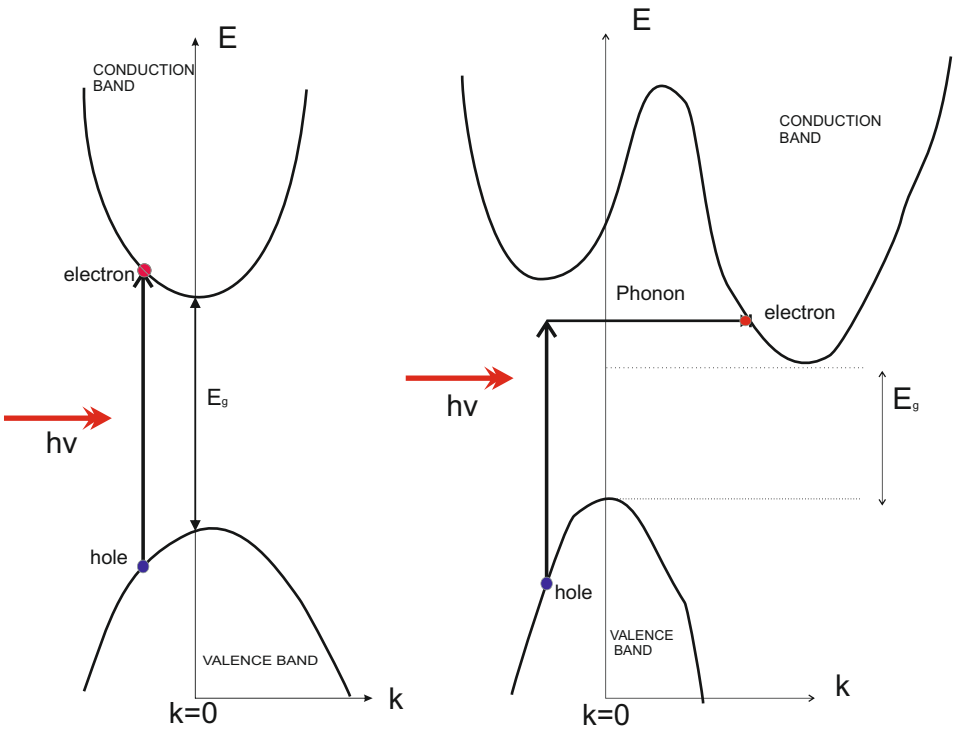

Figure 2.6: Scheme of photon absorption. On the left a direct optical transition and on the right an indirect one.

in this transition are [Dre01]:

1. Interband transitions are expected to have a threshold energy at the energy gap.

2. There are two possibilities for transitions due to absorption of light:

   (a) Direct optical transition (DOT): As it is possible to see in fig. 2.6 on the left, this kind of transition is a vertical transition. It does not involve changes in the wavevector of the initial and final state of the electron, but only a change in the energy. For energy conservation reasons, only photons can be involved in this process. In fact photons cause a negligible transfer of momentum.

   (b) Indirect optical transition (IOT): As it is possible to see in fig. 2.6 on the right, this kind of transition is not vertical. It involves a photon and a scattering event of the electron that leads to a momentum exchange. For example the scattering can happen with a phonon or with lattice imperfection.

3. Because of the Pauli Exclusion Principle, an interband transition can only occur from an occupied state below the Fermi level to an unoccupied state above the Fermi level.

4. Photons of a particular energy are more effective in producing an interband transition if the energy separation between the two bands is nearly constant over many wavevector values. In that case, there are many initial and final states which can be coupled by the same photon energy. Thus, the interband transitions is expected to be most important for wavevector values near band extrema. That is, in Fig. 2.7, is possible to see that states around $\mathbf{k} = 0$ make the largest contribution in the creation of excitons. It is also for this reason that optical measurements are so important in studying energy band gap.

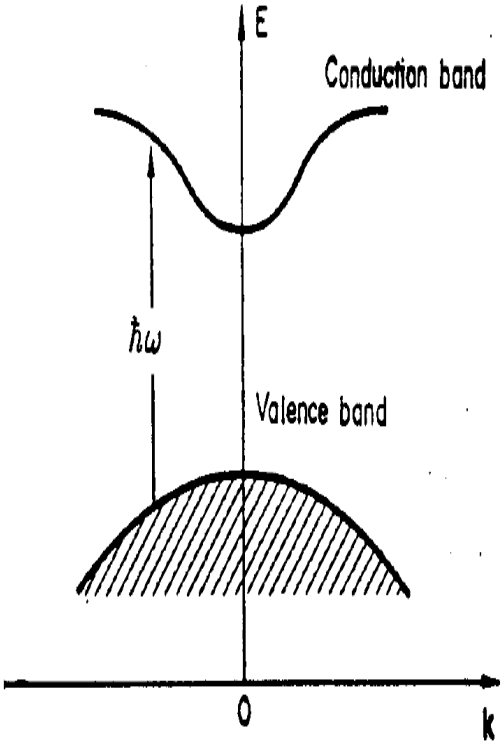

Figure 2.7: Schematic diagram of an allowed interband transition. Figure from [Dre01].

This properties are strictly related to the interband contribution to the conductivity. The conductivity tensor is related with the interband current density j_α which flows in the direction α upon application of an electric field E_β in direction

β by

$$j_\alpha = \sigma_{\alpha\beta} E_\beta \tag{2.29}$$

where $\sigma_{\alpha\beta}$ is a tensor writable as

$$\sigma_{\alpha\beta} = \frac{e^2}{m^2} \sum_{i,j} \frac{|f(E_i) - F(E_j)|}{E_i - E_j} \frac{\langle i| p_\alpha |j\rangle \langle j| p_\beta |i\rangle}{-i\omega + 1/\tau + (i/\hbar)(E_i - E_j)}. \tag{2.30}$$

The sum in Eq. 2.30 is over all valence and conduction band states labelled by i and j. Structure in the optical conductivity arises through a singularity in the resonant denominator of Eq. 2.30 as discussed in the first and the last point of the list of properties above (see 2.2.1). The appearance of the Fermi functions $f(E_i) - f(E_j)$ follows from the Pauli principle in property (3) of 2.2.1. The dependence of the conductivity on the momentum matrix elements $\langle i| p_\alpha |j\rangle \langle j| p_\beta |i\rangle$ accounts for the tensorial properties of $\sigma_{\alpha\beta}$ and relates to the second point of the list 2.2.1.
Once the conductivity is determined, is possible to evaluate the permittivity and the dielectric function of the material and have a quite satisfactory knowledge of the optical properties of the studied system (see section **??**.

2.2.2 Nonlinear polarization contribution

Nonlinear optics is the field of optics that describes the response of light in nonlinear media, that is, media in which the incoming electric field of the light create a dielectric polarization response which is nonlinear [Boy08]. Typically a high electric field, for example the field generated by a laser source, is needed to excite this kind of response in the material. In the case of linear optics, as seen in eq. 2.5, the polarization depends linearly on the applied field. In the nonlinear case this dependence has to be generalized and the polarization expressed as a power series in the field strength

$$\mathbf{P} = \epsilon_0(\chi^{(1)}\mathbf{E} + \chi^{(2)}\mathbf{E}^2 + ...) \tag{2.31}$$

Doing this the n-th order of the polarization can be written as [She84]

$$\begin{aligned}\mathbf{P}^{(n)}(\mathbf{r},t) = \int_0^\infty dt_1 \dots dt_n \int_{-\infty}^\infty \epsilon_0 \chi^{(n)}(\mathbf{r}-\mathbf{r}_1,\dots,\mathbf{r}-\mathbf{r}_n, t-t_1,\dots,t-t_n)\cdot \\ \mathbf{E}(\mathbf{r}_1,t_1)\dots\mathbf{E}(\mathbf{r}_n,t_n) d\mathbf{r}_1 \dots d\mathbf{r}_n\end{aligned} \tag{2.32}$$

where the susceptibility $\chi^{(n)}$ is a tensor of rank n which depends on the symmetry of the medium and on the intensity of the applied field. The first relevant term is the second order of the polarizability, which, in case of two incoming electric fields $E(t) = E_1 e^{-i\omega_1 t} + E_2 e^{-i\omega_2 t}$, results into five different terms:

$$
\begin{aligned}
P^{(2)}(t) = \epsilon_0 \chi^{(2)} \big[& 2E_1^* E_1 + 2E_2^* E_2 + && \text{(OR)} \\
& + E_1^2 e^{-i(2\omega_1)t} + E_2^2 e^{-i(2\omega_2)t} + c.c. \big] && \text{(SHG)} \\
& + 2E_1 E_2 e^{-i(\omega_1+\omega_2)t} + c.c. + && \text{(SFG)} \\
& + 2E_1 E_2^* e^{-i(\omega_1-\omega_2)t} + c.c. + && \text{(DFG).}
\end{aligned}
\tag{2.33}
$$

In this equation the first two terms are the Optical Rectification (OR) terms, the two next are the Second Harmonic Generation term (SHG) and the last two are the Sum Frequency Generation term (SFG) and the Difference Frequency Generation term (DFG) respectively. The OR terms correspond to generation of a quasi-DC polarization, the SHG terms correspond to the creation of components of the polarization which contain the double of the incoming beam frequency, the SFG term corresponds to the creation of a component with the sum of the incoming beams frequencies and DFG corresponds to the creation of a component with the difference of the incoming beams frequencies. Usually, only one of these components will be measurable, because the nonlinear polarization can efficiently produce an output signal only if the phase-matching condition, equivalent to the momentum conservation, is matched. In therms of the momenta it means that

$$
\mathbf{k}(\omega_3) = \mathbf{k}(\omega_1) + \mathbf{k}(\omega_2) \tag{2.34}
$$

is satisfied. This condition in literature is often called 3-wave-mixing and can also be expressed as

$$
\mathbf{\Delta k} = \mathbf{k}(\omega_1) + \mathbf{k}(\omega_2) - \mathbf{k}(\omega_3) = 0. \tag{2.35}
$$

Practically, the desired non-linear process is chosen selecting the polarization of the incoming radiation and the orientation of the crystal.

2.2.3 Sum Frequency Generation

For the measurements performed in this work, the relevant process is SFG. There are different reasons that makes this technique interesting. In fact this method is specifically used to analyze surfaces and interfaces because has an intrinsic surface sensitivity for material that are non centrosymmetric: indeed in centrosymmetric materials the second order contribution of the susceptibility is zero for reasons of symmetry and, when this happens, the second order term of the polarization vanishes. Since the bulk of gases, liquids and most solids are centrosymmetric media, the contribution of SFG in the bulk is almost always missing. On the other hand, at an interface between two different materials, the inversion symmetry is broken and for this reason also the centrosymmetricity, such that a SFG signal can be generated here. SFG has one other advantage: the measures with this technique

can be performed in air, water or via other media. This means that this spectroscopic method is versatile and, for this reason, suitable for biological interfaces.

The basic principles behind the generation of the SFG signal will be explained. A laser beam of frequency ω_1 interacts in the crystal with a laser beam of frequency ω_2 generating a nonlinear polarization $\mathbf{P^{(2)}}(\omega_3)$ of frequency $\omega_3 = \omega_1 + \omega_2$ as in figure 2.8.

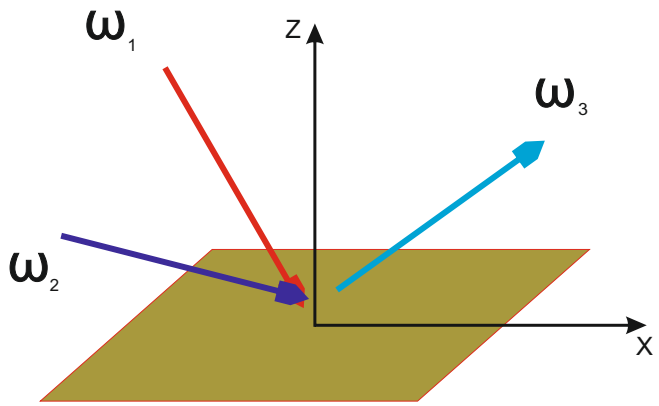

Figure 2.8: Scheme of a typical SFG experiment.

This nonlinear polarization can be interpreted as a collection of dipoles that oscillates at the new frequency and thereby acts as a radiation source at this frequency. As discussed in the precedent section, both energy and momentum conservation are required. So there is a preferential phase matching direction where the momentum conservation is satisfied. In other words eq. 2.35 is the condition for perfect phase matching. When this condition is fulfilled, the generated wave maintains a fixed phase relation with respect to the nonlinear polarization and the generated signal is maximum. Microscopically, it means that the individual atomic dipoles constituting the material system are properly phased so that the field emitted by each dipole adds coherently in the forward direction [Boy08]. When eq. 2.35 is not satisfied, the intensity of the emitted radiation is lower. In this case the intensity of the sum-frequency signal at the exit plane of the nonlinear medium is given by [Boy08]

$$I_3 = I_3^{max} \frac{sin(\Delta kL/2)}{\Delta kL/2} \tag{2.36}$$

and this expression predicts a dramatic decrease in the effeciency of the SFG signal if Δk is different from zero. Here L is the effective path length through the crystal.

SFG signal is used to do spectroscopic analysis of materials. Commonly is used as a vibrational spectroscopic technique. In this method two laser beam hit a surface and the SFG signal is detected producing information on the surface properties. Typically in a SFG experiment, one of the beams has a fixed wavelength (upconverting beam) and the other is a tunable laser (resonant beam). By tuning the resonant beam one activates vibrational resonances. In the most used setup of vibrational SFG the upconverting beam is in the visible frequency range, while the resonant beam is in the infrared. In the case of electronic resonant SFG used for the measure of this work, the beams are a visible supercontinuum as resonant beam and a visible light as upconverting beam (see ref to experimental part when i will have done it).

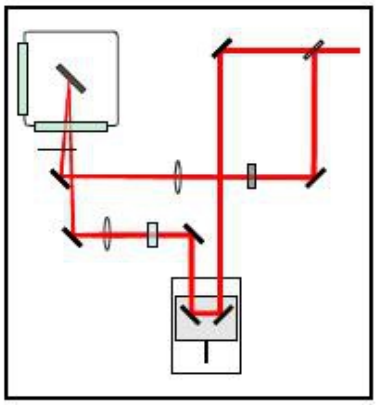

Figure 2.9: Pump-Probe experimental setup.

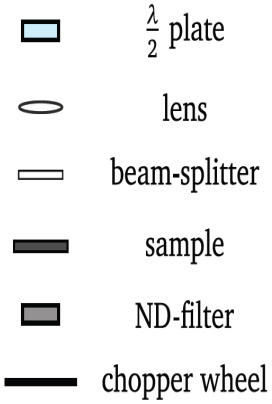

Figure 2.10: legend

2.3 Time-resolved techniques

Light can be used not only as a probe tool, but also as a pump perturbation for driving a system into a required state. This allows to utilize time-resolved experiments with the so-called pump-probe technique. With this method light is used to populate and to detect the state of a system [KZ90]. A first laser pulse is used to optically pump the sample; then a second laser pulse is used to probe the system. Is possible to set the delay between the two pulses using a stage that can be moved, changing the optical path of one pulse relative to the other as shown in figure 2.9.

This configuration provides one pump and one probe beam. One of these beam is sent to a retro-reflector mounted on a linear motorized translation stage, whose purpose is the control of the delay between pump and probe pulse. By setting the delay, it is possible to have exact temporal snapshot spectra of what happens in the excited state, a sort of film of the temporal evolution of the state. Usually the probe pulse is weaker than the pump in order to avoid a subsequent probe-induced-change of the measured property.

Transient absorption spectroscopy is an example of a pump-probe technique.

Figure 2.11 shows a scheme of a transient absorption measurement. In this figure is depicted the intensity of transmitted light as a function of the delay between pump and probe pulse. A first sudden change, due to the excitation of electrons, is observed at t = 0 and is followed by a long-lasting exponential decay. At $\Delta t = 0$ pump and probe arrive at the same time and the measured signal is

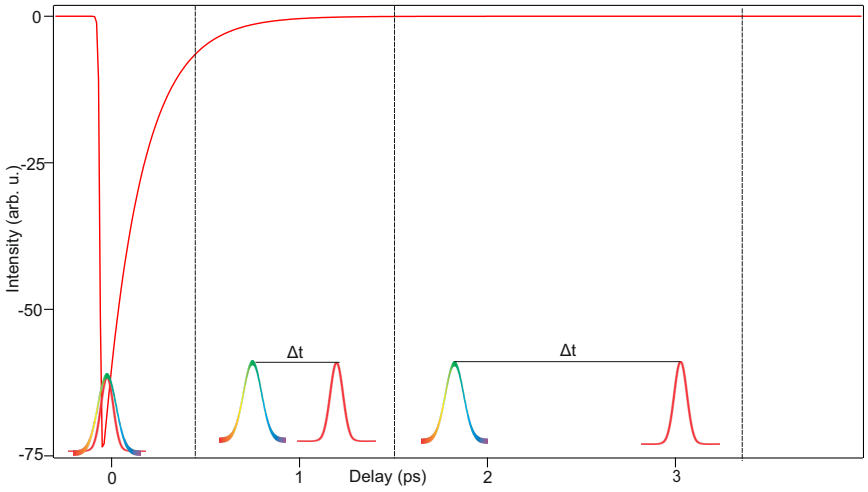

Figure 2.11: Transient absorption measure and scheme of the pump probe pulses.

due to the instantaneous effects of the excitation, which in this case correspond to an increase of the absorption due to electronic transition. At positive delays, the system begins the process of relaxation. Every data point corresponds to a different pair of pump and probe pulses. Usually the changes induced and measured by each of the pulses are independent of the effects induced by the previous light pair because the system comes back to the unperturbed state within the time interval between two pulse pairs. The duration of the pulse determines the time resolution of the experiment. The relative ratio between the free carrier excitation and light absorption due to resonant processes determines the intensity and the sign of the transient absorption signal.

Many different behaviors can be expected depending on the properties of the materials and on the used pump and probe frequency. This gives the possibility to look at different important processes as, for example, chemical reactions that are initiated by light (photoinduced chemical reactions), transfer of excitation energy between molecules, parts of molecules, or molecules and their environment and the behavior of electrons that are free from a molecule or crystalline material.

2.4 Experimental Setup

2.4.1 Laser System

The laser that we have used, is a femtosecond pulsed laser. To have such a short pulse is not a random choice. In fact what we do, is to investigate excited levels of a system, and, to obtain a good resolution, is necessary to have such short pulses. Indeed when an excited level is populated, we are interested in looking what happens suddenly after the excitation and so a femtosecond pulse is needed, because the relaxation of the level happens in the femto-pico second range. With a pulsed laser of less than 40 femtosecond, is possible to have a good resolution. A consequence of the fact that the pulse duration is so short is that the peak power is high.
This property makes pulsed lasers ideal for experiments in which a high photo-excitation and time resolution is required. The laser system used in our experiment is a commercial setup from the company Coherent. It is based on a mode-locked Ti:Sapphire oscillator (Micra) and a regenerative amplifier (RegA). In the next two sections these components will be explained.

2.4.2 Mode locked Ti:Shappire oscillator

A laser, to be operative, has to be composed at least by these three basic components: a gain medium, a pumping mechanism and a cavity delimited by a partial reflector on one side, and a total reflector on the other. The gain medium is a material that amplifies light by stimulated emission. This means that if light of a determined wavelength passes through the gain medium, the power of that light is increased.

Normally, when light passes through a material it is absorbed. On the other hand if in precedence an inversion of population has been created with the pump source, which means that an excited level is filled with electrons coming from the ground state, when light with proper wavelength comes, is possible to have stimulated emission and amplification of the signal. This amplification is possible because the photons created in this way have same phase, direction, polarization, and frequency of the incoming photons. The gain medium in the Micra is a Sapphire (Al_2O_3) crystal doped with Titanium (Ti) atoms. The range of absorption for this crystal is between 400 and 600nm, while it emits from 680 to 1100nm and has a maximum at 790nm. Lasing is permitted only if a strong population inversion between the two levels involved in the stimulated emission is reached. For this purpose, energy has to be transferred to the system in order to move the atoms to their excited states. This process, which is the pumping, is possible in Ti:Sapphire with the help of another intense laser source. In the Micra design light

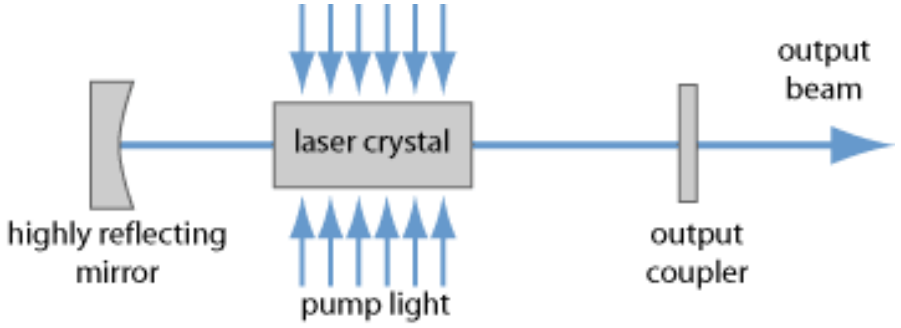

Figure 2.12: Setup of a optically pumped laser
The laser resonator is made of a highly reflecting curved mirror and a partially transmissive flat mirror, the output coupler, which extracts some of the circulating laser light as the useful output. The gain medium is a laser crystal, which is pumped, e.g. with light from a flash lamp.Figure from http://www.rp-photonics.com/lasers.html.

at 532nm (green) is used, generated by the second harmonic of a diode pumped solid state laser ($Nd:YVO_4$, Coherent Verdi).

The most common lasers produce a continuous wave as an output and can operate at the desired wavevector satisfying the condition $k = 4\pi/nd$, where d is the length of the cavity and n is an integer number. The wavevectors (or the waves) that satisfy this condition are called longitudinal modes of the cavity. It is also possible to obtain pulsed laser. What is done in the laboratory is to fix the phase relationship between the different oscillating modes of the resonant cavity. The laser is then said to be phase-locked or mode-locked. The constructive and destructive interference between different modes makes possible for the laser light to be produced as a train of pulses. This process is reached in Ti:Sapphire in a passive way, thanks to the electro-optical Kerr-effect. The Kerr effect is a nonlinear optical effect occurring when intense light propagates in crystals and glasses. It is physically originated by a nonlinear polarization generated in the medium, which itself modifies and influence the propagation properties of the light. All these induced changes can be described as a modification of the refractive index. In particular, the refractive index changes according to $\Delta n = n_2 I$ where n_2 is the nonlinear index and I is the optical intensity. The intensity I have also a nonlinear shape because is a Gaussian, thus the more intense part of the beam is focused stronger and the process is self-sustaining. Furthermore, high intensities are required for the Kerr-lens to be formed and this can only happen upon interaction with a mode-locked pulse.

When the intensity for the activation of the Kerr effect is reached, another non linear process is induced, this time caused by the temporal changes in the intensities and not by the spatial distribution. This process is called self-phase modulation (SPM): an initial unchirped optical pulse acquires a so-called chirp, i.e. a temporally varying frequency. This time dependent phase change caused by SPM is associated with modification of the optical spectrum. For example for a Gaussian beam with beam radius R in a medium with length d, the phase change per unit optical power is described by the proportionality constant

$$\gamma = \frac{4n_2 d}{\lambda R^2} \tag{2.37}$$

In general, if the initial pulse is unchirped or positively chirped, SPM leads to spectral broadening (an increase in optical bandwidth), and if the initial pulse is negatively chirped, spectral compression can result (always assuming a positive nonlinear index). In our system a positive chirp is induced.

This spectral broadening is compensated by a prism compressor in the resonator. Typically, a prism compressor is made of two dispersive prisms. The dispersion of the prism material causes different wavelength components to travel along different paths. The compressor is built such that all wavelength components leave the compressor at different times, but in the same direction. Using this properties in the right way permits to generate a negative chirp in the pulse, which compensates the positive one caused by the optical components. For every loop in the cavity, a part of the light is coupled out of the resonator through the partial reflector. The repetition rate of the oscillator is therefore related to the length of the cavity d by $1/\tau = c/2d$. Typically, the repetition rate of the Micra is set to 80MHz but values between 76MHz and 82MHz are possible. The output power is specified to be major of 300mW [Coh07] and in our case it is around 500 mW.

2.4.3 RegA

For the employment of non-linear processes such as frequency doubling, high output power of pulses are needed: it turns out that the output power of the Micra is not sufficient for the experiments we perform. What is necessary is a way to amplify the pulses. For doing that we use a commercial device, the RegA, also from Coherent [Coh97]. In this instrument, like in the Micra, the active medium is a $Ti : Al_2O_3$ crystal pumped by the remaining Verdi output.
A high speed acousto-optic modulator made of Tellerium Dioxide (TeO2), the cavity dumper, is used to couple in and out the pulses coming from the oscillator. The basic idea is to keep the optical losses of the laser resonator as low as possible

for some time (about 21 round trips), so that an intense pulse builds up in the resonator and then to extract this pulse within about one cavity round-trip time using a kind of optical switch. After this time the population inversion in the Ti:Sapphire is completely depleted. To regenerate this high population inversion needed for amplification, spontaneous emission has to be avoided. For this purpose a quality switch (Q-switch) is used. With this component is possible to modulate the intracavity losses of the laser resonator. The resonator losses are kept at a high level. As lasing cannot occur at that time, the energy is fed into the gain medium by the pumping mechanism and accumulates there. When the population inversion is completely regenerated, the quality of the resonator is restored and a new pulse is coupled in.
The high power of the generated pulse can cause changes in the pulse profile due to non-linear effects and can damage the active medium. To avoid these undesired effects, the chirped pulse amplification (CPA) technique is used. With this method the laser pulse is stretched out temporally prior to the amplification in the RegA. This stretch is obtained thanks to a particular sequence of dispersive gratings. In our setup, the pulse is positively chirped and stretched in time up to 50 to 100 ps. Therefore its intensity becomes sufficiently low to make safe amplification possible. Also the Q-switch is responsible for a upchirp caused to the pulse during each round-trip of the amplification. Therefore an analogous set of gratings is used after amplification to remove the chirp and re-compress the pulse.

2.4.4 Signal

As explained in the theoretical part, our experimental methods need at least two different beams to be sent on the samples in order to have time resolved measurements and to create the SFG signal.

As it is possible to see in figure 2.13, the 800nm RegA output is compressed at the grating compressor and then is splitted by a 50% partially reflecting mirror and from here two different beams are created: beam A and beam B (see figure 2.13).

Beam A is directed to an Optical Parametric Amplifier (OPA) which amplifies the signal and permits us to set the desired frequency. This beam will become the pump beam. At the output of the OPA we obtain a pulsed beam centered at 1.8 eV and with power of the order of 40 mW. This beam passes trough a system of gratings to avoid the group velocity dispersion. In our case, what we want as a pump is a 3.6 eV pulse because of the energy level alignment of the SP6 molecule. For obtaining this energy, the pump beam passes through a BBO crystal which is an excellent non-linear crystal for frequency-doubling of visible and near IR laser light [Nik91]. After this the beam is sent to the delay stage, with

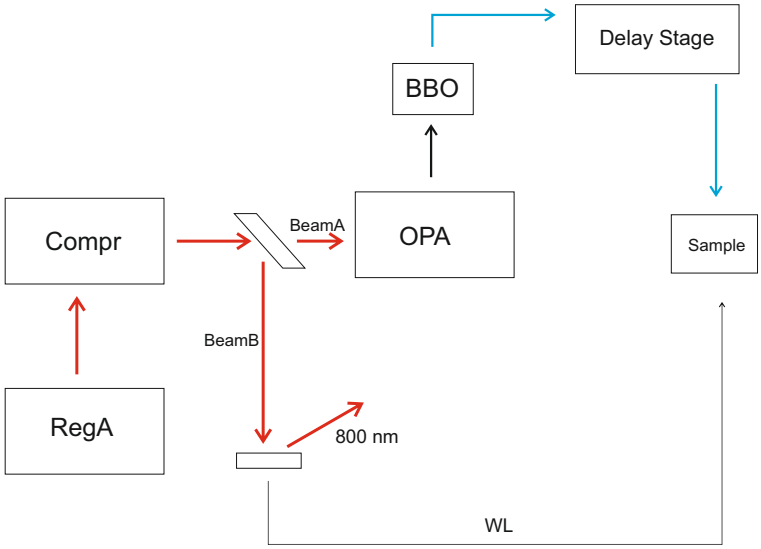

Figure 2.13: Experimental setup
For a more accurate desciption see the text below.

which is possible to control the delay between the pulses. By moving the stage of a distance d, the optical path changes by 2d and therefore the pulse is delayed by a time $t = 2d/c$ where c is the speed of light. After these steps there is the possibility to use a neutral density (ND) filter to attenuate the intensity obtained. The beam is then focused onto the sample thank to a 300 mm lens. For the transmission experiment the angle of incidence of this beam is between 5 and 10 degree.

On the other hand, beam B is tubed and then divided into two beams thanks to a partially reflecting mirror. One of the two beams with 90% of the initial beamB power, is maintained as an 800 nm beam and the remaining 10% is used to form the probe beam, transforming it in a white light continuum (WLC) generated by self-phase modulation in sapphire. This WLC has a large spectral phase which can be compensated by applying an opportune distortion to a deformable mirror. Was shown that the white-light pulses can be compressed to reach a duration of circa 10 fs [WBB$^+$11]. This beam is then sent and focused on the sample.

The transmitted light is collected by a photodiode and a lock-in amplifier is used to measure the signal. For this reason the signal has to be modulated before reaching the sample. A rotating optical chopper is used to modulate the signal in particular the pump pulse. The blade of the chopper has two homocentric series of hole,

permitting to chop the beam at different frequency. The lock-in amplifier is then set to detect at the difference frequency between the frequency of the pump and the probe. In this way only the pump induced signal is detected and it is possible to have a clean signal, because of the high value of the signal to noise ratio.

2.4.5 UHV chamber and sample holder

Our samples are held in an Optistat CF-V cryostat from Oxford Instruments. This cryostat is mounted on an x, y, z translational stage on the optical table and is fixed by a self-made support. The stage permits to align along the three translational degrees of freedom. For the rotational degrees is sufficient to tight the screws of the support at the desired angle.

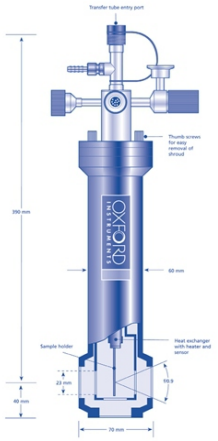

Figure 2.14: Cryostat
Figure
http://www.cryospares.co.uk/ProductDetails.asp?ProductCode=FTOPTICFV

The cryostat is shown in figure 2.14. It is a continuous flow cryostat, which means that it has no internal tank for storing the cryogenic liquid and the sample is in vacuum. The cryogenic liquid is provided from an external tin through an insulated transfer tube and is delivered to the heat exchanger. The gas coming back from the heat exchanger is used to cool the radiation cover of the cryostat and then flows along the flexible section of the transfer tube to the exhaust port, thereby preserving the incoming liquid from thermal radiation. Both liquid helium and nitrogen can be used. The first makes possible to maintain temperatures of circa $4.2°K$ while using liquid nitrogen allows to reach temperatures down to about $77°K$. Nevertheless the measurements of this work were all performed without cooling.
The sample is fixed to a sample holder, which is directly screwed on the bottom

of the heat exchanger of the cryostat by a retaining screw. A groove in the cold finger prevents the sample holder from rotating during adjustment. Is possible to set the angular alignment with respect to the windows when the cryostat is closed. Eight different positions are possible: parallel to each of the four windows or forming a 45° angle with respect to a couple of windows. The sample holder has been designed from the group and produced at the mechanical workshop of the Fritz Haber Institute.

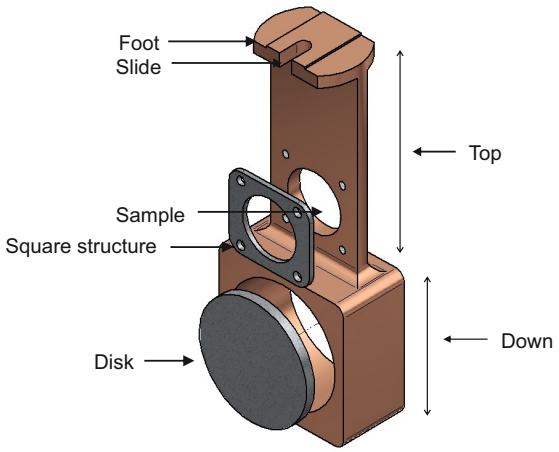

Figure 2.15: Sample holder description of SH

Figure 2.15 sketches the sample holder. With reference to this figure, there are two main parts: the top part and the down part. The top part is used to hold the samples while the down part is used for the references.

The samples are fixed to the holder with the aid of the square structure present in figure 2.15. The references are mounted on the disk which can be screwed in the hole present in the down part of the structure. As references is possible to use also 1 inch mirrors, which are fixed with two screwed rings on the down part of the structure. The main part of the sample holder is made with copper, while the rings, the disk, and the square structure are made of stainless steel. The foot presents an extrusion, which adapts with the groove in the cryostat heat exchanger, and a slide, where the retaining screw is inserted. This permit to change the distance between the windows and the sample. The latest is secured between the top structure and the squared structure. There is the possibility to insert a gold film in between of the sample holder and the cold finger, to improve the thermal contact.

2.4.6 Characterization of the sample

(Probably i will add also the samples with 3.2 and 6.4 nm thickness if we will use it). In this work two samples are analyzed. One is composed by SP6 deposed on sapphire and the other is composed by SP6 deposed on ZnO($10\bar{1}0$). Both the samples have different thicknesses of SP6 deposed on it, one of 1.6 nm and the other one of 12 nm as is possible to see in figure 2.16 for the case of SP6/ZnO. In the figure is shown that two different substrates of ZnO are present, each one cut along the crystal face ($10\bar{1}0$). One substrate is epitaxially grown on the other. The profile structure of the other sample is equal to the one in the figure 2.16, but instead of the ZnOs, it has a substrate made of sapphire.

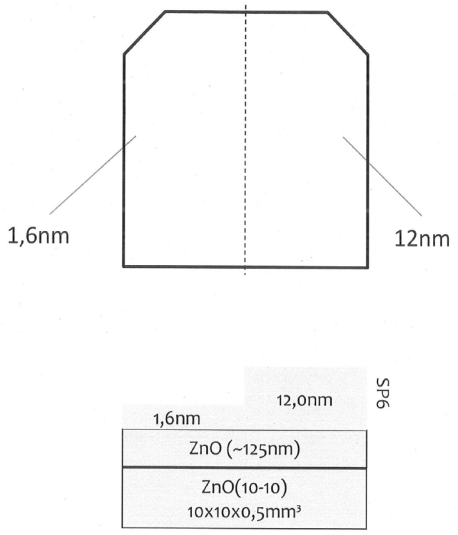

Figure 2.16: Sample:
SP6/ZnO thickness profile.

The SP6 and the 125 thick ZnO are deposed on the substrates by means of molecular beam epitaxial deposition (MBE). The relevant aspect of MBE is that the deposition rate, typically slow, allows the films to grow epitaxially. For this reason the overlayer composition and morphology can be precisely controlled.

Bibliography

[AM76] Ashhcroft, Neil W. ; Mermin, N. D.: *Solid State Physics*. Cengage Learning, 1976

[Ami12] Amin, Gul: *White LEDs Printed on Paper*, Linkping University, Diss., 2012. http://liu.diva-portal.org/smash/get/diva2:515790/FULLTEXT01

[BG00] Bassani, Franco ; Gassano, Umberto ; stellatum coelum (Hrsg.): *Fisica dello stato solido*. Bollati Boringhieri, 2000

[BGK+01] Borisov, A. G. ; Gauyacq, J. P. ; Kazansky, A. K. ; Chulkov, E. V. ; Silkin, V. M. ; Echenique, P. M.: Long-Lived Excited States at Surfaces. In: *Phys. Rev. Lett.* 86 (2001), Jan, 488–491. http://dx.doi.org/10.1103/PhysRevLett.86.488. – DOI 10.1103/PhysRevLett.86.488

[Boy08] Boyd, Robert: *Nonlinear Optics*. 3rd ed. Academic Press., 2008

[BSH08] Blumstengel, S. ; Sadofev, S. ; Henneberger, F.: Electronic coupling of optical excitations in organic/inorganic semiconductor hybrid structures. In: *New Journal of Physics* 10 (2008), 065010. http://dx.doi.org/10.1088/1367-2630/10/6/065010. – DOI 10.1088/1367–2630/10/6/065010

[BSX+06] Blumstengel, S. ; Sadofev, S. ; Xu, C. ; Puls, J. ; Henneberger, F.: Converting Wannier into Frenkel Excitons in an Inorganic/Organic Hybrid Semiconductor Nanostructure. In: *Phys. Rev. Lett.* 97 (2006), S. 237401

[Coh97] Coherent (Hrsg.): *RegA Model 9000 Laser Operator's Manual*. Coherent, 1997

[Coh07] Coherent, Inc (Hrsg.): *Micra Laser Operator's Manual*. Coherent, Inc, 2007

[DBD02] Dulub, Olga ; Boatner, Lynn A. ; Diebold, Ulrike: STM study of the geometric and electronic structure of ZnO(0001)-Zn, (000-1)-O, (10-10), and (11-20) surfaces. In: *Surface Science* 519 (2002), Nr. 3, 201 - 217. http://dx.doi.org/10.1016/S0039-6028(02)02211-2. – DOI 10.1016/S0039–6028(02)02211–2

[Dre01] Dresselhaus, M. S.: *Solid State Physics part II Optical Properties of Solids*. Fall, 2001

[EBC+04] Echenique, P.M. ; Berndt, R. ; Chulkov, E.V. ; Fauster, Th. ; Goldmann, A. ; Hfer, U.: Decay of electronic excitations at metal surfaces. In: *Surface Science Reports* 52 (2004), Nr. 78, 219 - 317. http://dx.doi.org/http://dx.doi.org/10.1016/j.surfrep.2004.02.002. – DOI http://dx.doi.org/10.1016/j.surfrep.2004.02.002. – ISSN 0167–5729

[Fog11] Foglia, Laura: *Transient reflectivity and coherent phonon excitation: An ultrafast probe of the metal-to-insulator transition in VO2*, Fritz-Haber-Institut der Max-Planck-Gesellschafft, Abt. Physikalische Chemie, Diplomarbeit, 2011. http://www.fhi-berlin.mpg.de/pc/electrondynamix/publications/diplom/foglia_diplom2011.pdf

[Fre31] Frenkel, J.: On the Transformation of light into Heat in Solids. I. In: *Phys. Rev.* 37 (1931), Jan, 17–44. http://dx.doi.org/10.1103/PhysRev.37.17. – DOI 10.1103/PhysRev.37.17

[Gad95] Gadzuk, J.W.: Resonance-assisted, hot-electron-induced desorption. In: *Surface Science* 342 (1995), Nr. 13, 345 - 358. http://dx.doi.org/http://dx.doi.org/10.1016/0039-6028(95)00607-9. – DOI http://dx.doi.org/10.1016/0039–6028(95)00607–9. – ISSN 0039–6028

[HSF+00] Hoffmann, M. ; Schmidt, K. ; Fritz, T. ; Hasche, T. ; Agranovich, V.M. ; Leo, K.: The lowest energy Frenkel and charge-transfer excitons in quasi-one-dimensional structures: application to MePTCDI and {PTCDA} crystals. In: *Chemical Physics* 258 (2000), Nr. 1, 73 - 96. http://dx.doi.org/http://dx.doi.org/10.1016/S0301-0104(00)00157-9. – DOI http://dx.doi.org/10.1016/S0301–0104(00)00157–9. – ISSN 0301–0104

[HYZ11] Huang, Jia ; Yin, Zhigang ; Zheng, Qingdong: Applications of ZnO in organic and hybrid solar cells. In: *Energy Environ. Sci.* 4 (2011), 3861-3877. http://dx.doi.org/10.1039/C1EE01873F. – DOI 10.1039/C1EE01873F

[KFZ+10] Klingshirn, Claus ; Fallert, J. ; Zhou, H. ; Sartor, J. ; Thiele, C. ; Maier-Flaig, F. ; Schneider, D. ; Kalt, H.: 65 years of ZnO research - old and very recent results. In: *physica status solidi (b)* 247 (2010), Nr. 6, S. 1424–1447. http://dx.doi.org/10.1002/pssb.200983195. – DOI 10.1002/pssb.200983195

[Kit05] Kittel, Charles: *Introduction to solid state physics*. 8th. John Wiley & Sons,Inc, 2005

[KZ90] Khundkar, L R. ; Zewail, A H.: Ultrafast Molecular Reaction Dynamics in Real-Time: Progress Over a Decade. In: *Annual Review of Physical Chemistry* 41 (1990), Nr. 1, 15-60. http://dx.doi.org/10.1146/annurev.pc.41.100190.000311. – DOI 10.1146/annurev.pc.41.100190.000311

[LL60] Landau, L.D. ; Lifshitz, E.M.: *Course of theoretical physics*. Bd. 8: *Electrodynamics of continuous media*. Pergamon press, 1960

[Moe01] Moench, Winfried: *Semiconductor Surfaces and Interfaces*. Springer, 2001

[Nik91] Nikogosyan, D.N.: Beta barium borate (BBO). In: *Applied Physics A* 52 (1991), Nr. 6, 359-368. http://dx.doi.org/10.1007/BF00323647. – DOI 10.1007/BF00323647. – ISSN 0947–8396

[She84] Shen, Y.R. ; Sons, John Wiley (Hrsg.): *The Principles of Nonlinear Optics*. Wiley-Interscience Pubblication, 1984

[St07] Sthler, Julia: *Electron Transfer and Solvation Dynamics at D2O- and NH3-Metal Interfaces*, Freie Universitt Berlin, Diss., 2007

[Ter84] Tersoff, J.: Theory of semiconductor heterojunctions: The role of quantum dipoles. In: *Phys. Rev. B* 30 (1984), S. 4874–4877

[W07] Wöll, Christof: The chemistry and physics of zinc oxide surfaces. In: *Progress in Surface Science* 82 (2007), 55 - 120. http://dx.doi.org/10.1016/j.progsurf.2006.12.002. – DOI 10.1016/j.progsurf.2006.12.002

[Wan37] Wannier, Gregory H.: The Structure of Electronic Excitation Levels in Insulating Crystals. In: *Phys. Rev.* 52 (1937), Aug, S. 191–197. http://dx.doi.org/10.1103/PhysRev.52.191. – DOI 10.1103/PhysRev.52.191

[WBB+11] Wegkamp, D. ; Brida, D. ; Bonora, S. ; Cerullo, G. ; Stahler, J. ; Wolf, M. ; Wall, S.: Phase retrieval and compression of low-power white-light pulses. In: *Applied Physics Letters* 99 (2011), Nr. 10, 101101. http://dx.doi.org/10.1063/1.3635396. – DOI 10.1063/1.3635396

[ZYM09] Zhu, X.-Y. ; Yang, Q. ; Muntwiler, M.: Charge-Transfer Excitons at Organic Semiconductor Surfaces and Interfaces. In: *Accounts of Chemical Research* 42 (2009), Nr. 11, 1779-1787. http://dx.doi.org/10.1021/ar800269u. – DOI 10.1021/ar800269u. – PMID: 19378979